5-2015

Clinical Microendoscopy for the Mapping of Tumor Margins using a Support Template for Near-Continuous Imaging

Chantal Marie Soobhanath
University of Arkansas, Fayetteville

Clinical Microendoscopy for the Mapping of Tumor Margins using a Support Template for Near-Continuous Imaging

An Honors Thesis submitted in partial fulfillment of the requirements of Honors Studies in Biology

By

Chantal Soobhanath

2015

Biology

J. William Fulbright College of Arts and Science

The University of Arkansas

ACKNOWLEDGEMENTS

I would like to thank my thesis director, Dr. Timothy Muldoon for the opportunity to conduct my research in his laboratory and for his continued assistance. I would also like to thank Sandra Prieto, Amy Powless and Gage Greening for being my mentors throughout the two years spent conducting research in Biomedical Engineering.

This work was made possible through funding by a research grant provided by the Honors College at the University of Arkansas**.** Clinical trials were facilitated through a collaboration with the University of Arkansas for Medical Sciences (UAMS). Sincere thanks to Dr. Jonathan Laryea and Dr. Jason Mizell for their assistance in providing patients, and to Dr. Keith Lai for providing histopathology slides and correlation data.

TABLE OF CONTENTS

1. INTRODUCTION.....4
2. METHODS.....11
    - 2.1 Clinical fiber bundle microendoscope instrumentation.....11
    - 2.2 Clinical trial at the University of Arkansas for Medical Sciences (UAMS).....12
    - 2.3 Acrylic Template.....15
    - 2.4 Correlation of DSLR to Microendoscope Images to Histopathology.....17
    - 2.5 Creating a Mosaic.....19
3. RESULTS.....20
    - 3.1 Acrylic Template.....20
    - 3.2 Quantitative correlation of DSLR to Microendoscope Images to Histopathology.....22
    - 3.3 Qualitative correlation of microendoscopy images to histopathology.....23
    - 3.4 Mosaicking.....24
4. DISCUSSION.....26
5. REFERENCES.....30

1. INTRODUCTION

Colorectal cancer is the third most common cancer in men and women and the second leading cause of cancer-related death in the United States [1]. There are nearly one million new cases of colorectal cancer diagnosed and half a million deaths world-wide each year [2]. Most colorectal cancers arise from benign, adenomatous polyps which initially form in the mucosa of the colon or rectum and protrude into the lumen of the intestine. Although adenomatous polyps are the precursor for colorectal cancer, not all colonic polyps are adenomas and 90% of adenomas do not progress to cancer [3]. Typically, polyps that grow to a large size and have a villous appearance or contain dysplastic cells are those that are most likely to become cancer [2].

Colonic adenomas are particularly dangerous because they are asymptomatic [3] and often go unnoticed until the disease has substantially progressed. Many are commonly found by means of endoscopic imaging studies performed because of unrelated symptoms [3]. Approximately 10% of large adenomatous polyps, if left untreated, become severe dysplasia (pre-cancerous polyps) and then eventually spread into the basement membrane where it then becomes classified as a malignant adenocarcinoma. As such, the American Cancer Society recommends that persons 50 years and older who have a normal risk for colorectal cancer undergo routine screening by colonoscopy beginning at age 50 and every 10 years thereafter. Strong evidence exists that screening for colorectal cancer reduces the incidence and mortality of the disease [4]. Approximately 90% of those diagnosed with early stage cancer live 5 or more years [5].

Colorectal cancer is most frequently diagnosed among persons between the ages of 65 and 74, with this group representing 23.9% of all diagnoses [4]. It is characterized

by symptoms such as rectal bleeding, abdominal pain, changes in bowel habits, anemia, and occult bleeding [6]. The conventional diagnostic test for this disease is white light colonoscopy with biopsy which involves the removal of tissue samples from the affected area for histopathology. However, since this technique employs white light illumination, it is limited to the observation of reflected visible light from the mucosal surface [7]. Additionally, histopathology evaluation creates a significant delay in diagnosis [7]. These issues have driven the need to develop a method which will enhance or improve the ability of colonoscopy to detect regions of dysplasia that are not visible with conventional white light endoscopy in real-time. Recent technological advances in fiber optics have stimulated the development of optical imaging methods that will allow in vivo analysis of surface epithelial tissue. Collectively, these imaging methods are known as optical biopsy, and they will enable physicians to delineate the edges of tumors, also known as tumor margins, during surgical procedures, without the need for frozen section or traditional paraffin embedded histopathology techniques.

Currently, many wide-field endoscopic imaging techniques exist that allow rapid visualization of a large surface area for identifying tumors and guiding biopsies. One such technique is autofluorescence endoscopy. Autofluorescence endoscopy allows imaging of endogenous fluorophores in tissue, such as collagen, NADH and flavin, as well as chromophores such as hemoglobin which absorb visible light [8]. When any fluorescent molecule is excited by a short-wavelength light source, the fluorophores are excited and emit light of longer wavelength. The light emitted can be seen as a fluorescence emission which enables any changes to the surface mucosa to be analyzed (Figure 1). Autofluorescence images display differences in the distribution and

concentration of fluorophores and chromophores in the tissue, as well as differences in mucosal thickness. These differences are denoted by varying degrees of fluorescence, which appear on an artificially colorized image that is displayed to a clinician, and can be used to characterize regions of pre-malignant and dysplastic tissue. Elevated tumors have a thicker mucosa and therefore they absorb more light and appear magenta, a complementary color of green, on the image that the clinician observes [8]. Normal mucosa appears bright green due to the fluorescence of the fluorophores in the tissue. Autofluorescence imaging therefore allows for the detection of regions of flat or depressed colonic adenomas that do not have sufficient morphological changes to be observably detected by traditional white light endoscopy [8].

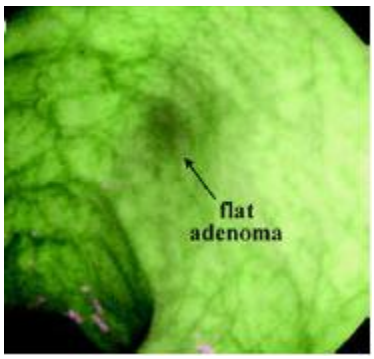

Figure 1: Autofluorescence endoscopy showing a flat colonic adenoma. Adapted from [8]

While this technique is highly sensitive and produces a large number of true positives, it yields a low specificity, meaning that it produces a large number of false positives when compared to the total number of healthy individuals. This is potentially due to the presence of benign changes in the tissue, such as ulcerations or inflammation, which are detected as adenomas by the autofluorescence endoscope, since they appear dark green due to an increased amount of hemoglobin (which absorbs visible light) present in these areas of the tissue.

Wide-field endoscopy does not allow for the visualization of the tissue morphology of the epithelial surface and is limited to the observation of reflected visible light from the mucosal surface [7]. Therefore, several microendoscopic imaging devices have been developed to combat this limitation by providing a real-time analysis of tissue histology. One such device is the confocal endomicroscope which aims at providing the physician with a method for in-vivo imaging of living tissue [9, 12]. This device has been applied to in-vivo imaging of human skin tissue [10], oral mucosa [11], and gastrointestinal mucosa [12]. Confocal microendoscopy is an imaging method which allows for high-resolution imaging and depth-sectioning of gastrointestinal mucosa. This system also works in conjunction with fluorescent imaging techniques to provide a method for observing subcellular detail, thereby providing instantaneous histopathology during ongoing endoscopy [12].

The confocal endomicroscope employs two consecutive pinholes through which emitted light from tissue fluorescence must pass through in order to be detected. These pinholes function to remove out-of-focus light and to provide only in-focus light to the camera, thus producing high resolution images. One type of commercially available confocal endomicroscope is called the Optiscan/Pentax which uses a miniaturized scanning head to raster scan laser light across the distal tip of a fiber bundle to enable confocal fluorescence imaging of the tissue (Figure 2). The images obtained closely resemble conventional histopathology and have the added feature of depth analysis of the tissue. Although this system can obtain high resolution images of tissue in real time, the distal tip of the endoscope is larger than 12mm and efforts to miniaturize the confocal

endomicroscope leads to compromised image resolution due to fiber bundle pixelation [13].

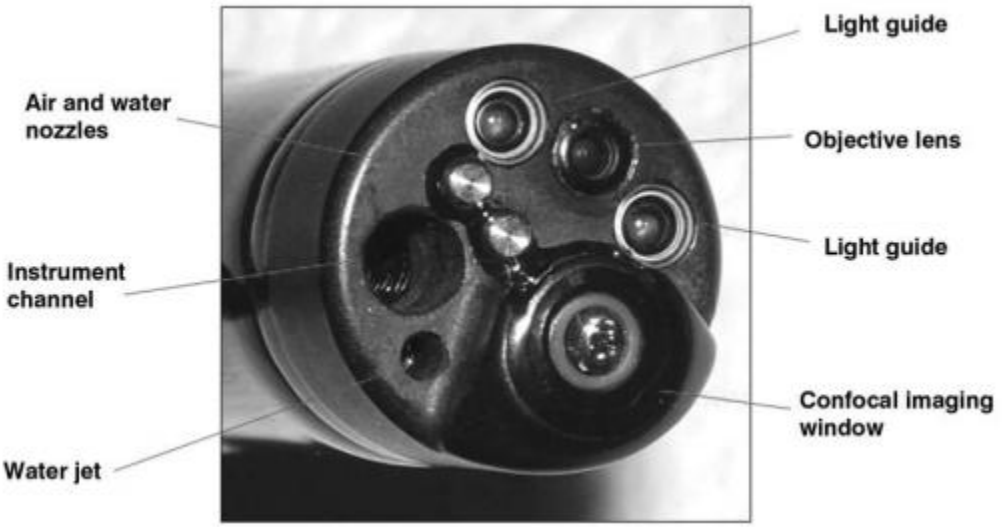

.

Figure 2: The distal tip of the confocal endomicroscope showing the miniaturized scanning head for raster scanning of laser light. Adapted from [12].

Therefore, an alternative to these microendoscopic imaging methods, called a clinical fiber-bundle microendoscope, has been developed. This device may be useful to provide physicians with a procedure for early screening of suspicious lesions, and point-of-care assessment of the tumor margins prior to surgical resection of adenocarcinomas. This device employs a fiber optic image guide which allows visualization of cells on the epithelial layer of the tissue specimens in real time. It will enable physicians to make informed decisions by providing a method that will allow for the differentiation of dysplastic and non-dysplastic cells. It will also allow physicians to visualize regions of occult dysplasia which may not be otherwise visible. This is critical to increase early detection, decrease mortality, and allow further investigation such as biopsies or removal of occult dysplasia. The low cost of the clinical microendoscope will allow increased

availability in clinics worldwide, especially in developing countries and in low socioeconomic communities in the United States, and will provide a reduced cost of screening procedures. This will provide the public with an incentive to be screened for colorectal cancer without worrying about the hefty cost that they will need to endure.

The clinical fiber bundle microendoscope was constructed by our team at the Translational Biophotonics and Imaging Laboratory. This system consists of a fiber optic image guide with a 1 mm active diameter, an 8-bit USB CMOS camera, and custom LabVIEW which allows the user to adjust gain and exposure prior to and during image acquisition. The entire system runs off of a laptop, making it convenient for use in the clinic, and is currently approved for imaging freshly resected surgical samples of colorectal tissue at the University of Arkansas for Medical Sciences (UAMS) in Little Rock, AR. In order to visualize the cells of the epithelium during imaging, proflavine dye is topically applied to a section of the tissue. Proflavine is an acridine-derived dye which intercalates DNA and predominantly stains the nucleus of the cells [14]. Its peak fluorescence emission of around 525nm occurs when excited by light at a wavelength of approximately 455nm, which allows distinct visualization of the morphology of the cells and the surrounding tissue. Uptake of proflavine has been found to be near-instantaneous, with imaging possible within a few seconds and lasting for several minutes [15].

Using the clinical microendoscope, the epithelium of tumors can be viewed by bringing the fiber bundle in direct contact with the epithelial surface. The blue epi-fluorescent light that is emitted from the distal end of the fiber optic image guide excites proflavine and causes cells to fluoresce. Tumor margins can then be distinguished by examining specific quantitative characteristics of cells, such as gland size and gland

circularity, and qualitatively analyzing any abnormalities. The tumor margin refers to the location in which the cells transition from cancerous to normal. It defines the area that must be resected during surgical procedures in order to successfully remove the tumor [16].

The clinical microendoscope will enable surgeons to view the tumor margin along various chosen axes. To facilitate the acquisition of quality, high-resolution images, the distal end of the fiber bundle needed to be stabilized using a secure fixture in order to prevent motion blur due to unsteady manual placement of the image guide. Therefore, my role in this project was to design and fabricate a custom support template to effectively position and stabilize the image guide to reduce integration time and prevent motion blur, as well as provide a template for discrete positioning of the fiber bundle to aid in correlation to histopathology. When the image guide was stabilized, the gain of the camera could be reduced, which in turn reduces noise and pixilation, thereby producing clearer images. Exposure can also be increased until room light becomes a significant noise contributor. The template was constructed using optically clear cast acrylic (McMaster Carr) and allowed near continuous imaging along a chosen axis. This ensured that overlapping images could be acquired for later image mosaicking, which can provide a larger field of view for tissue analysis. Once images are acquired, they are then correlated with the histopathology for the imaged section and a diagnosis can be made.

2. METHODS

2.1 Clinical fiber bundle microendoscope instrumentation

The clinical fiber bundle microendoscope is an effective tool that allows us to view cells on the epithelial layer of the tissue specimens in order to characterize regions of dysplasia and specifically map tumor margins. The system (Figure 3) consists of a blue LED (455 nm/40 nm FWHM) light source (Philips, USA), a filter set (Chroma Tech, USA) consisting of a 525nm/40nm emission bandpass filter, a 460nm short pass excitation filter, a dichroic mirror with a cutoff wavelength of 475nm, an 8-bit USB CMOS camera (Flea 3 USB3.0, Model FL3-U3-32S2M-CS, Point Grey Research, Inc., Canada), a 60mm tube lens (Thorlabs, USA), a 10x, 0.25 NA objective (Olympus, Japan), and a circular fiber bundle image guide with a 1mm active diameter consisting of 50,000 individual fibers approximately 4.5 microns in diameter (FIGH-50-1100N fiber, Myriad Fiber Imaging Tech., Inc., USA). The distal end of the fiber bundle image guide includes a SubMiniature Version A (SMA) connector which is designed to reduce friction between the fiber bundle edges and the epithelial tissue during imaging, as well as to protect the delicate glass surface of the fiber bundle from chipping. This setup is run using a laptop and LabVIEW imaging software to acquire images rapidly.

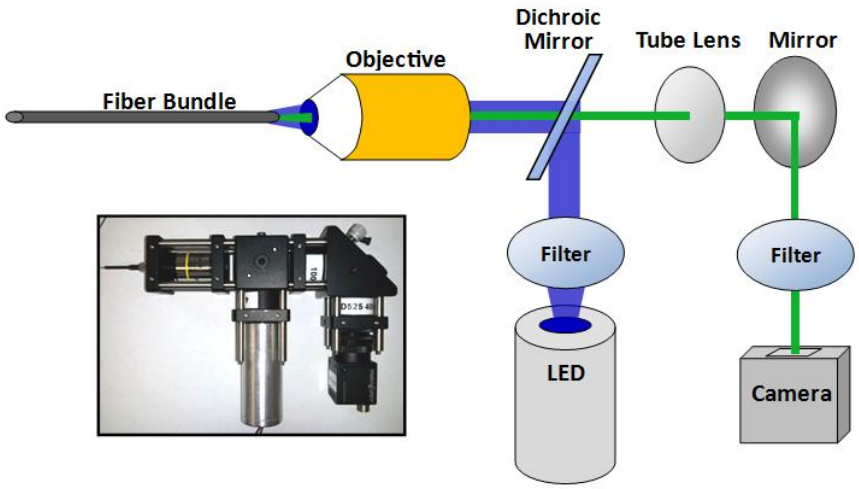

Figure 3. Schematic of the microendoscope system showing the blue light emitted from the LED and the green light that is collected from the fluorescing tissue and passed on to the camera. Photograph of unenclosed system, inset. Adapted from [17].

2.2 Clinical trial at the University of Arkansas for Medical Sciences (UAMS)

2.2.1 Overview

A clinical trial at the University of Arkansas for Medical Sciences (UAMS) was first initiated in April, 2014 under an Institutional Review Board (IRB) approved protocol (IRB #202224). Adult patients over the age of 18 who had a known colorectal invasive adenocarcinoma were recruited for the study. Although patients with a history of prior treatment (chemotherapy and/or radiotherapy) were initially excluded from the study, the protocol was amended to include these patients in order to observe treatment associated changes in epithelium. Colorectal tissue specimens were obtained from nine screened and approved patients, who had signed an informed consent before surgery, and these were used for imaging with the clinical microendoscope system (Table 1)

Case	Diagnosis
1	Invasive colonic adenocarcinoma
2	Invasive colonic adenocarcinoma
3	Invasive rectal adenocarcinoma
4	Invasive colonic adenocarcinoma
5	Invasive rectal adenocarcinoma
6	Tubular adenoma
7	Invasive colonic adenocarcinoma
8	Invasive colonic adenocarcinoma
9	Invasive colonic adenocarcinoma

Table 1: Summary of cases and patient diagnoses

Prior to imaging, colorectal tissue was surgically removed at the Department of Colorectal Surgery at UAMS. The freshly resected tissue was taken to the pathology lab where it was washed to remove superficial debris, longitudinally sectioned to expose the lumen, and finally pinned onto a paraffin block. Three pins were placed along a section of the tumor (Figure 4) in order to delineate the line of imaging for further histopathology correlation.

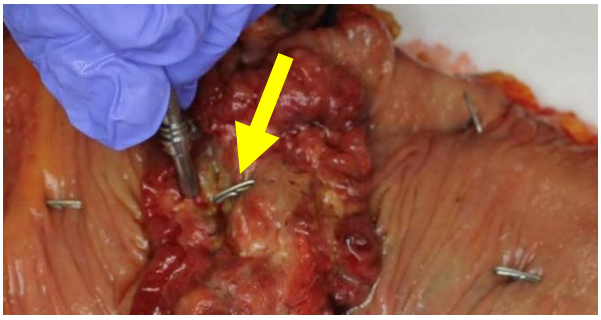

Figure 4: The fiber optic image guide of the clinical microendoscope is shown in contact with the tissue during imaging. The arrow points to one of the pins used to delineate the line of imaging

After this procedure, microendoscopy imaging was carried out for approximately twenty minutes in order to minimize changes to the tissue due to drying out (see section 2.2 Microendoscopy image acquisition). After imaging was complete, the tissue was submerged in 10% (v/v) formalin for protein fixation. A cross section of the imaged

region was then sliced (Figure 5) and placed into a cassette for paraffin embedding and hematoxylin and eosin staining. Diagnosis of the epithelial pathology was performed by the study pathologist (Dr. Keith Lai) at UAMS.

Figure 5: A sliced cross section of imaged region of colorectal tissue that was placed into a cassette for paraffin embedding and hematoxylin and eosin staining prior to diagnosis of the epithelial pathology.

2.2 Microendoscopy image acquisition

Once the colon was clean and stained, it was transferred to a bench and an initial image of the resected specimen was taken using a conventional digital camera (DSLR). A cotton swab was used to coat the epithelium with proflavine (0.01% w/v in phosphate buffered saline, PBS) to allow visualization of the cell structure. In order to ensure that the cells remained visible throughout the procedure, proflavine was reapplied as needed. The clinical microendoscope was powered on and the LabVIEW software was opened on the laptop. For all microendoscopy images acquired, the gain was set to either 0 or 5 dB, and the exposure to either 100 or 150 ms in LabVIEW. The DSLR was used to record the location of the fiber optic image guide as it was placed along the tissue and a ruler was used to demarcate the position from the starting point. Images were taken at 5mm intervals along the length of the tumor. Reference images of normal tissue were also taken for comparison during correlation. Cellular debris was removed from the fiber optic image guide as needed by washing in ethanol and wiping with lens paper.

2.3 Acrylic Template

2.3.1 Initial template design

An acrylic support template was designed to effectively position and stabilize the image guide to increase integration time, improve signal-to-noise ratio, and prevent motion blur due to unsteady manual placement of the fiber. This template also served as a tool for documenting the discrete positioning of the fiber bundle to aid in histopathology correlation. The initial design of the template featured a 12"L x 3"W x 1/4"H sheet of optically clear cast acrylic (McMaster-Carr, USA). The diameter of the SMA connector of the fiber optic image guide was measured using a vernier caliper. Once the size of the SMA connector was determined, 98 holes of 3mm diameter were drilled along the x-axis of the acrylic with a center-to-center spacing of 2.5mm to allow for near continuous imaging of the tissue. 22 holes of 3mm diameter and 2.5mm center-to-center spacing were also drilled along the y_1 and y_2 axes at 1.4941 inches and at 3.6713 inches from the leftmost edge of the acrylic (Figure 6). The acrylic was epoxied onto two metal posts that enabled the height of the template to be adjusted.

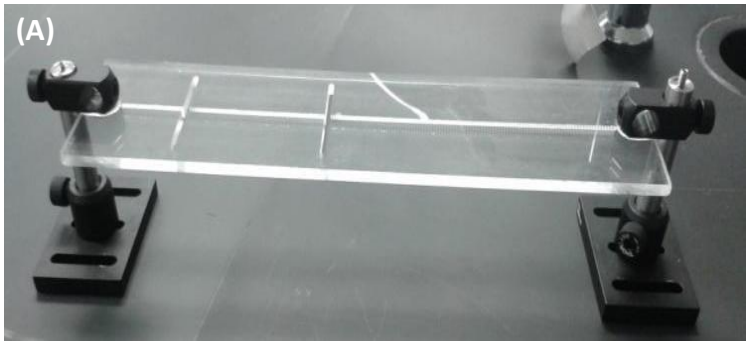

(B)

Optically clear cast acrylic	McMaster Carr
Right -Angled Post Clamp	RA90 - Right-Angle Post Clamp, Fixed 90° Adapter; ThorLabs
Bases	BA2 - Mounting Base, 2" x 3" x 3/8"; ThorLabs
Post Holders	PH1 - Ø1/2" Post Holder, Spring-Loaded Hex-Locking Thumb screw, L = 1", ThorLabs
Posts	TR3 - Ø1/2" Optical Post, SS, 8-32 Setscrew, 1/4"-20 Tap, L = 3"; ThorLabs

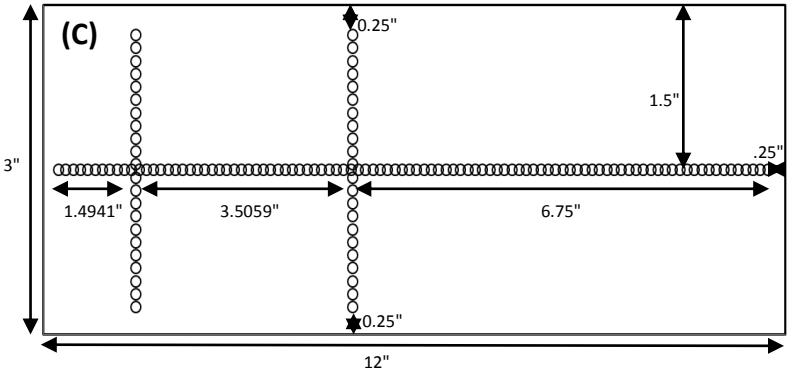

Figure 6: Acrylic support template. (A) Completed acrylic structure. (B) Table of parts used in constructing acrylic template. (C) Schematic of the initial acrylic template

2.3.2 Modified template design to include a silicone rubber structure

The initial template design was limited because it did not allow the SMA connector of the fiber optic image guide to make contact with the uneven epithelial surface of the tissue. The acrylic template was not allowed to come into contact with the colorectal tissue to prevent damage to the epithelial lining; therefore, with this template, images of valleys in the tissue could not be obtained unless they were acquired manually. Therefore, a new template was constructed which featured a continuous slot that was 0.25 inches in diameter that would allow the widest part of the SMA connector to fit into the template

(Figure 7). The fiber optic image guide was stabilized to prevent image blur during image acquisition using 1"W x 11"L x 1/8"H translucent silicone rubber (McMaster Carr, USA). The silicone rubber was cut down the center to allow secure fitting of the wire of the fiber optic image guide. It was held in a fixed position using a sheet of acrylic 3"W x 12"L x 1/4"H (McMaster Carr, USA) with a hole cut through the center to match the dimensions of the silicone rubber (Figure 6). With this new design, the template could be held at a fixed height and the fiber optic image guide could be adjusted vertically depending on the height of the tissue beneath.

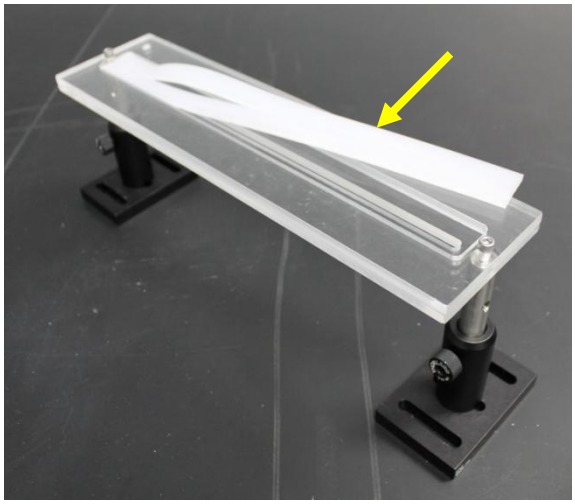

Optically clear cast acrylic	McMaster Carr
Bases	BA2 - Mounting Base, 2" x 3" x 3/8"; ThorLabs
Post Holders	PH1 - Ø1" Post Holder, Spring-Loaded Hex-Locking Thumb screw, L = 2", ThorLabs
Posts	TR3 - Ø1/2" Optical Post, SS, 8-32 Setscrew, 1/4"-20 Tap, L = 1.5"; ThorLabs
Silicone Rubber	Extreme-Temperature Silicone Rubber Translucent, Plain Back, 1/8" Thick, 12" x 12"; McMaster Carr

Figure 7: Modified acrylic design featuring two pieces of clear acrylic drilled with continuous slots of varying sizes. The arrow points to a strip of silicone rubber. The table shows the parts that were used to construct the acrylic support template

2.4 Correlation of DSLR to Microendoscope Images to Histopathology

Precise correlation of microendoscopy images with the location on the tissue was achieved by superimposing a series of DSLR images with each probe site onto one image

of the gross tissue. A colored oval was numbered and placed at the probe sites to map the correlated H&E locations, approximately to scale (Figure 8).

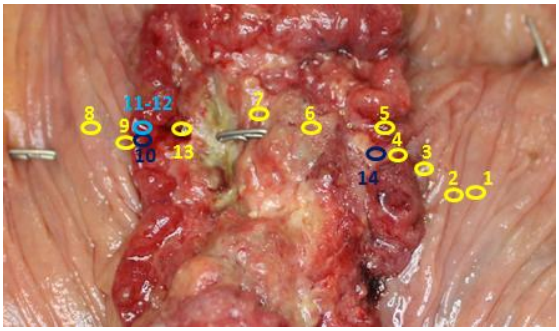

Figure 8: Correlation of DSLR images to precise location on ex-vivo tissue using colored ovals that were numbered and placed at the probe sites to map the correlated H&E locations.

Subsequently, DSLR images were matched to their exact microendoscopy images from the precise location on the tissue. Images of H&E slides along with the histopathology diagnoses at various points were provided by the study pathologist, Dr. Keith Lai at UAMS (Figure 9).

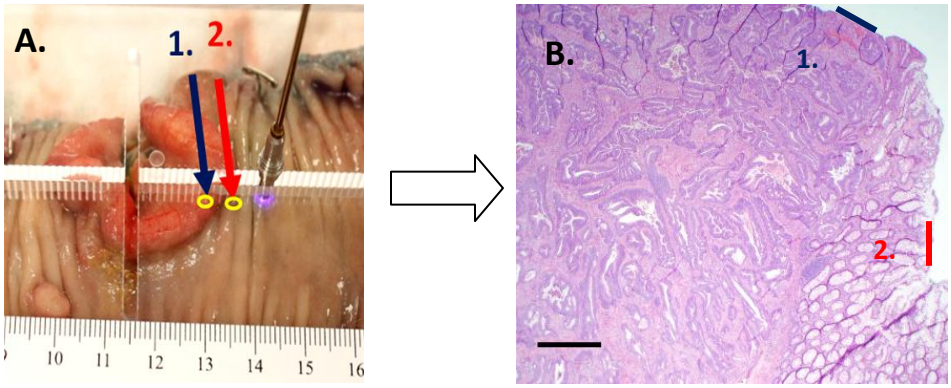

Figure 9: Correlation of DSLR images to histopathology. The addition of colored ovals to represent the location of the probe along the tissue (A). Scale bars were added along the H&E slide to represent the area that was covered by the probe during imaging (B). Scale bar represents 0.5mm.

2.5 Creating a mosaic

Semi-automated image mosaicking is a technique that is used to compile individual images with a limited field-of-view to create composite images with a larger field of view. For this project, image mosaicking was used to compile 1mm field-of-view images obtained from the clinical microendoscope to create a larger sub sectional image of the tissue specimen. Videos of sections of tissue were obtained from the clinical microendoscope and saved in .avi format. These were converted into individual .tiff files in MATLAB to procure numerous still images of the section of tissue. Blurry images were discarded and the remaining individual files were cropped and edited to exclude the outside ring of pixels/fibers that were unevenly illuminated and created artifacts in the mosaicking (Figure 10). This was done by applying element-by-element binary operation to two arrays with singleton expansion to mask everything but the image and to create a completely black background for optimal image quality. Our mosaicking code was modified from a pre-existing mosaicking tutorial available from Drexel University [18]. Two consecutive images were chosen for mosaicking, and two matching points were manually selected from each image. Through bi-linear interpolation, the algorithm re-shaped and overlapped the images. This was repeated for all of the .tiff images to obtain a larger field of view up to 10mm long.

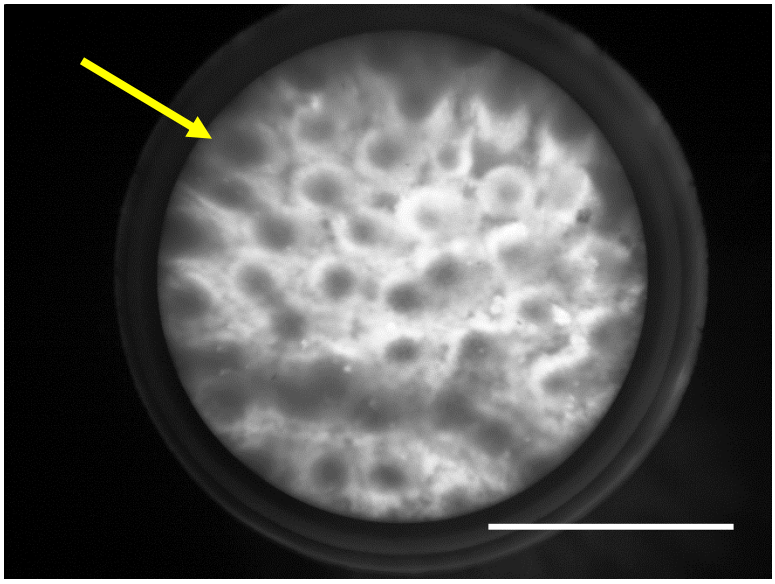

Figure 10: Microendoscopy image showing an arrow pointing to the outside ring of pixels/fibers that were unevenly illuminated and created artifacts in the mosaicking. Scale bar represents 0.5mm.

3. Results

3.1 Acrylic Template

3.1.1 Initial template design

The initial template design was used in obtaining images for subjects 2 and 3. The template stabilized the fiber optic image guide thus allowing high-resolution images to be obtained (Figure 11). Additionally, it allowed a reduction in the gain and an increased exposure time to be utilized. It was also an effective tool which allowed near-continuous imaging along both the x and y axes. However, the template did not allow the fiber optic image guide to acquire images of surface epithelium that was at a lower elevation than the tumor.

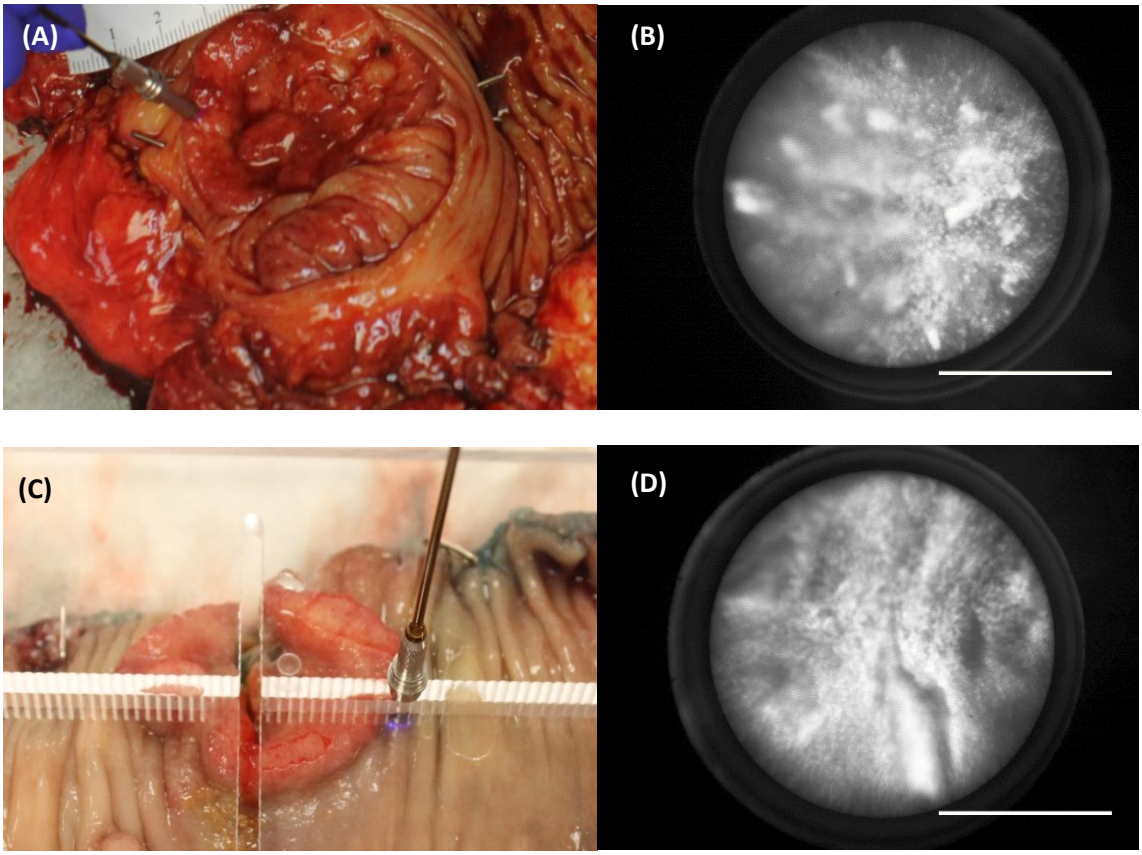

Figure 11: (A) Section of ex-vivo colorectal tissue showing the manual placement of the fiber optic image guide. (B) Microendoscopy image from the point site showing the blurry image obtained when the image guide was not stabilized. This image was taken with a gain setting of 5dB and an exposure of 100ms. (C) Section of ex-vivo colorectal tissue showing the position of the acrylic template with the fiber bundle image guide inserted along the x-axis. (D) Microendoscopy image from that point site showing a high-resolution image of invasive colonic adenocarcinoma that was captured with a gain of 0dB and an exposure of 150ms. Scale bars represent 0.5mm

3.1.2 Modified template design to include silicone rubber structure

The new template, which will be implemented in future cases at UAMS, will allow the fiber optic image guide to be stabilized and the probe to effectively take images along sections of the uneven tissue topography. After manual placement of the probe into the support template, the height of the fiber bundle can be adjusted until it touches the surface of the tissue and images can be acquired along the x-axis of the tissue (Figure 12).

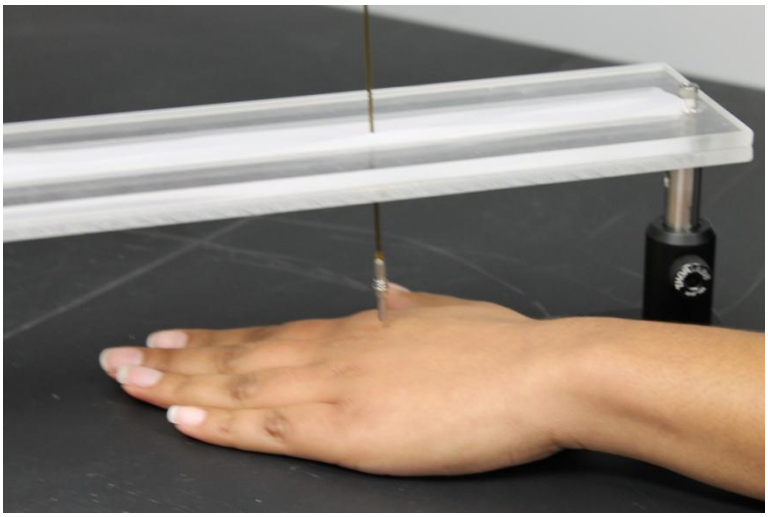

Figure 12: The fiber optic image guide is shown in contact with the hand while being supported in the new acrylic support template. The height of the image guide can be adjusted until it touches the surface of the tissue.

3.2 Quantitative correlation of DSLR to Microendoscope Images to Histopathology

The table below (Table 2) shows the quantitative results obtained after correlating the microendoscopy images with the histopathology. Many images were obtained using the microendoscope, however a significant number were unusable because they were either blurry or were repeated image sites.

Number of patients	9
Number of DSLR images acquired	498
Number of microendoscopy images acquired	498
Number of images actually used for correlation	49
Number of image sites correlated	19

Table 2: Quantitative correlation of microendoscopy to histopathology showing the number of images that were used for correlation.

3.3 Qualitative correlation of microendoscopy images to histopathology

The table below (Table 3) shows examples of microendoscopy images that were correlated to H&E.

Diagnosis	Microendoscopy Image	H&E Image
Normal	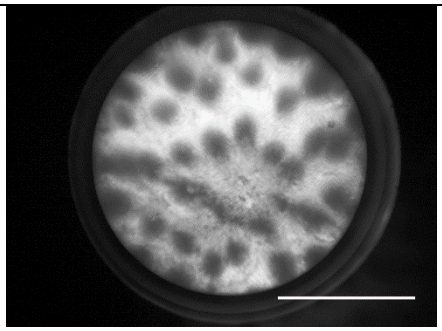	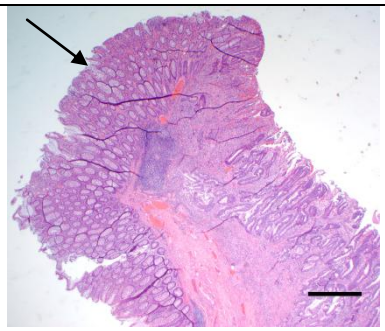
Invasive colonic adenocarcinoma	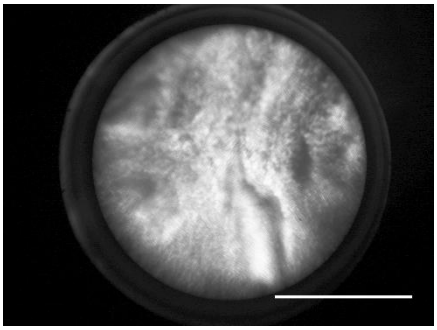	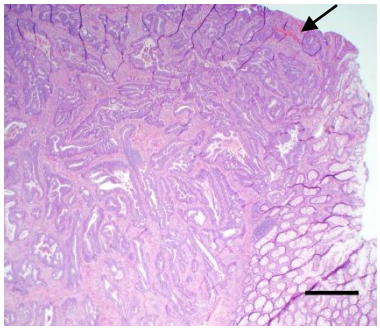
Invasive rectal adenocarcinoma	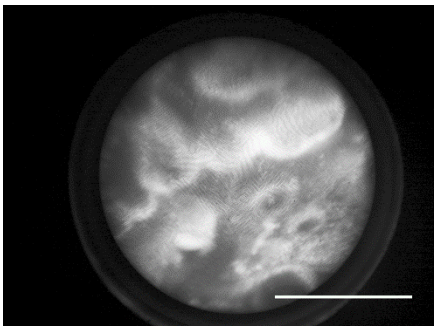	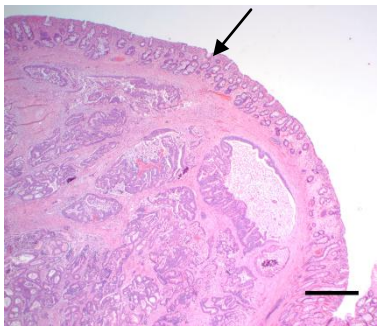
Tubular adenoma	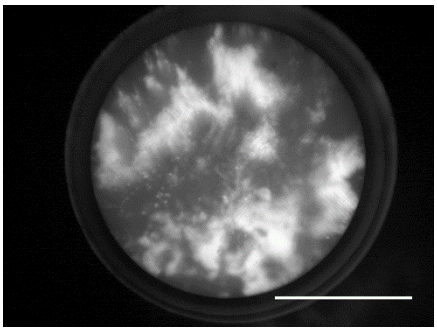	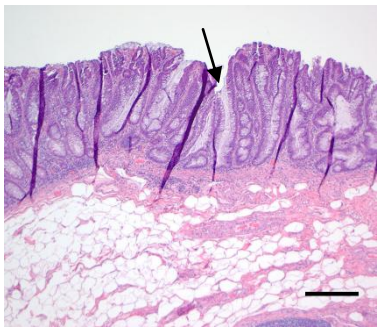

Table 3: Qualitative correlation of microendoscopy images to histopathology showing the various morphological features that characterize each type of cancer. Scale bars represent 0.5mm.

3.4 Mosaicking

Figure 13 shows examples of image mosaicking from 15 second video files, taken with the microendoscope, which covered areas up to 10 millimeters. The mosaics show comparisons of a hyperplastic polyp, invasive colonic adenocarcinoma, "normal" colon after adjuvant treatment, invasive rectal adenocarcinoma, and normal colon. The scale bars appear different for each mosaic since the current mosaicking code stretches the individual masked images in order to overlap them and leads to some larger and some smaller images. Therefore, individual scale bars were created for each mosaic.

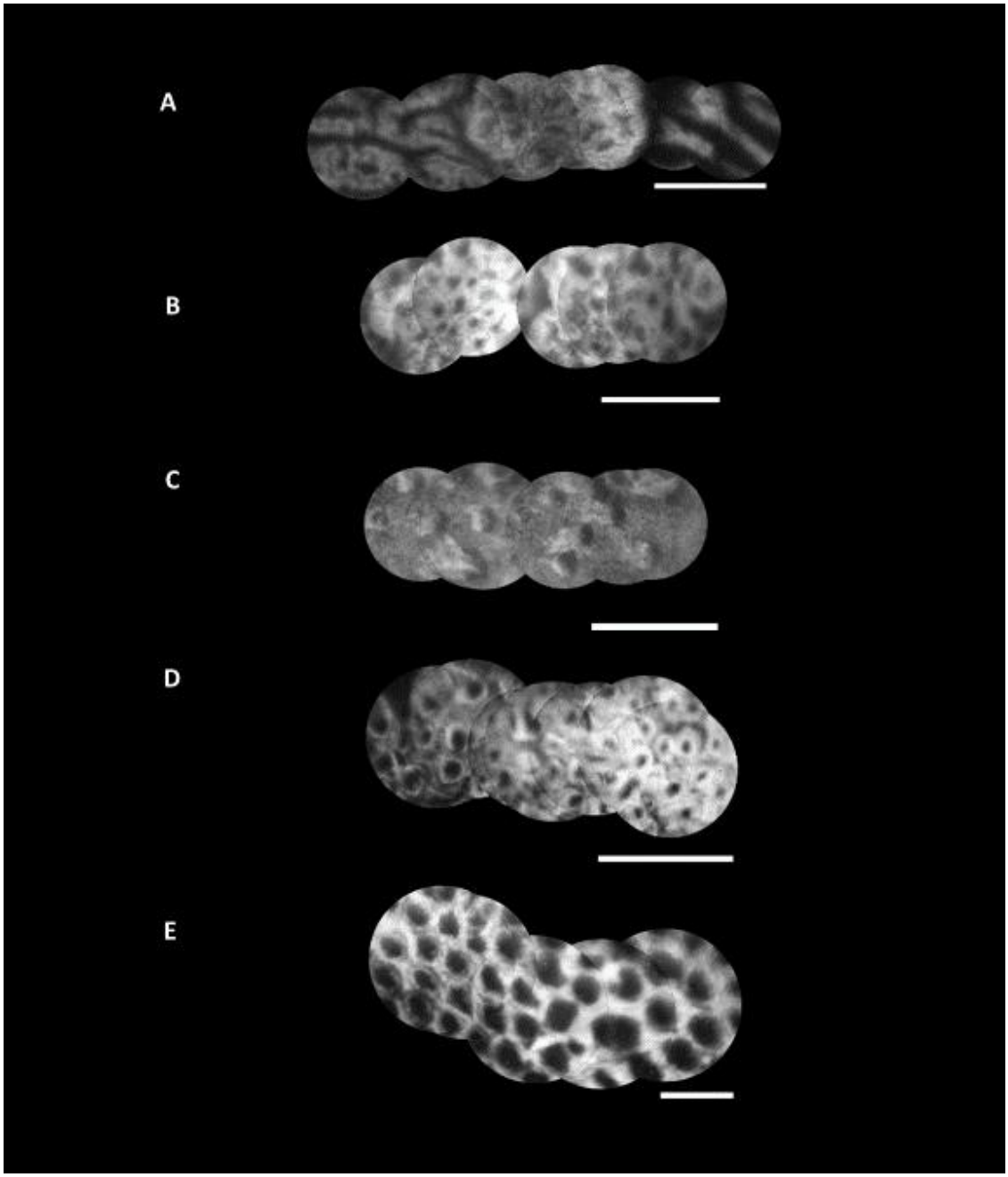

Figure 13: Image mosaics showing hyperplastic polyp (A), invasive colonic adenocarcinoma (B), "normal" colon after adjuvant treatment (C), invasive rectal adenocarcinoma (D), and finally normal colon (E). Images have been edited to enhance contrast and brightness for a better quality image. Scale bars represent 0.5mm

4. DISCUSSION

All of the outlined experiments were carried out to demonstrate the capabilities of the clinical fiber-bundle microendoscope as a viable alternative for non-invasive tissue analysis. Surface epithelium was detected using a fiber optic image guide and a custom LabVIEW interface designed to capture images on a computer. In effort to support the fiber optic image guide, an acrylic support template was constructed. The template effectively stabilized the fiber optic image guide and served as a tool for future correlation of microendoscopy images to histopathology.

While the fiber optic image guide was stabilized in the support template, the gain could be lowered to 0dB and the exposure could be increased to 150ms to increase signal-to-noise. Increased gain from the electronic amplification within the camera equally enhances the signal as well as noise components within an image. However, the best method used to capture a quality image is through the collection of more light from the sample. The best way to collect more light from a certain point in the sample is to increase the exposure time (signal). The more time that light is collected from the sample is the greater the probability of obtaining more photons of light from that area and thus a better pixel intensity could be obtained. This was achieved only when the image guide was stabilized since motion blur was avoided and as such, the gain could be lowered and the exposure could be increased. However, despite the usefulness of the acrylic template, it did not allow the tumor to be viewed along the XYZ axes. The template had to be turned each time in order to generate images along a new axis. This minor limitation did not create substantial problems in image acquisition since the template was sufficiently flexible to be rotated to acquire more images.

In the clinical study, a total of nine consented patients were used and 498 microendoscopy images were attained. However, despite this large number of images attained, only 49 images were usable. Many images attained represented the same image site and as such, a few images were selected to represent various imaging sites along the entire x-axis of the tumor. Some images were blurry so they were discarded.

The original template effectively stabilized the image guide but it was limited by its inability to allow the SMA connector of the fiber optic image guide to make contact with the uneven epithelial surface of the tissue. Therefore the design needed to be improved to include a rubber sheet which stabilized the fiber optic image guide and allowed its height to be adjusted to make contact with the epithelial layer of the tissue.

The clinical microendoscope allowed for the identification of regions of abnormal gland circularity. Through visualization of the microendoscopy images, normal glands could be viewed as circular structures while cancerous glands could be viewed as having a distorted shape. While the microendoscope did not allow characterization of the type of adenocarcinoma (something that could only be characterized through histopathology), it allowed for the detection of cancer as well as for the characterization of regions of occult dysplasia. Correlation of microendoscopy images to histopathology allowed for the validation of the clinical microendoscope so that an accurate diagnosis of cancer could be made. Correlation was facilitated through demarcating the precise location of the fiber bundle along a section of the tumor with a colored oval on an image of the gross specimen as previously described. The data was used to determine the location of the microendoscopy image as it related to the H&E slide. Correlational data from histopathology created a large collection of diagnoses of multiple types of cancer from

many individuals. Analysis of the features from each of these cancer types reveals similarities which can be used to validate that when the microendoscope acquires an image containing those features, that person has cancer. As such, the clinical microendoscope may be a useful adjunct tool for surgeons searching for regions of occult dysplasia during a colectomy procedure. Hyperplastic polyps and regions of occult dysplasia can also be found, using the clinical microendoscope.

This study was focused on qualitatively correlating microendoscopy images to histopathology through a focus on observing gland circularity. However, more quantitative methods could have also been employed to identify regions of dysplasia such as a measure of gland circularity. Normal tissue shows homogenous glands that are roughly circular. Abnormal and dysplastic cells have highly degenerate glands that are enlarged and non-circular. A measure of circularity and gland area are promising quantifiable microendoscopy image features which may correlate to regions of dysplasia.

While the clinical microendoscope is a viable alternative for minimally-invasive tissue analysis, it is limited by its inability to view tissue depth. Since the fiber bundle microendoscope does not perform optical sectioning, it is limited to imaging only the superficial 10-20 microns. Depth sensitivity may be improved by collecting light which has been diffusely scattered beneath the surface of the tissue. This method is currently an active area of research being targeted by members of the Translational Biophotonics and Imaging Laboratory.

Another limitation of the clinical microendoscope is the very narrow field of view of 1mm that can be obtained using the fiber optic image guide. Image mosaicking therefore provides a resource to overcome this limitation. Mosaicking has been

previously investigated by other researchers in the field [18] and allows the formation of compiled images depicting a larger field of view, thereby enabling physicians to better characterize regions of occult dysplasia prior to resection. Future work will be carried out to automate this mosaicking code since currently, the code requires manual selection of similar points on each image. This manual selection does not always prove accurate and the images become distorted when overlapped. Additionally, image mosaics were blurry and had to be enhanced for brightness and contrast since the video files were manually acquired. The new acrylic support template will allow the image guide to be stabilized, thus allowing acquisition of higher quality videos and more effective image mosaicking.

Overall, the clinical microendoscope is a functional tool to guide physicians during screening techniques for colorectal cancer. This system aims to augment traditional white light colonoscopy by enabling real-time analysis of histopathology, thus allowing a rapid diagnosis to be made. After substantial validation of the system, it will be useful for detecting regions of pre-cancerous and cancerous cells, including regions of occult dysplasia, which is critical for increasing early detection, and decreasing mortality from colorectal cancer.

References

1. Schoen, Robert E., et al. "Colorectal-cancer incidence and mortality with screening flexible sigmoidoscopy." *New England Journal of Medicine* 366.25 (2012): 2345-2357.
2. Boyle, Peter, and Maria Elena Leon. "Epidemiology of colorectal cancer."*British medical bulletin* 64.1 (2002): 1-25.
3. Levine, Joel S., and Dennis J. Ahnen. "Adenomatous polyps of the colon." *New England Journal of Medicine* 355.24 (2006): 2551-2557.
4. Zauber AG, Lansdorp-Vogelaar I, Knudsen AB, Wilschut J, van Ballegooijen M, Kuntz KM. Evaluating test strategies for colorectal cancer screening: a decision analysis for the U.S. Preventive Services Task Force. Ann Intern Med 2008;149:659–69.
5. Howlader N, Noone AM, Krapcho M, Garshell J, Miller D, Altekruse SF, Kosary CL, Yu M, Ruhl J, Tatalovich Z,Mariotto A, Lewis DR, Chen HS, Feuer EJ, Cronin KA (eds). SEER Cancer Statistics Review, 1975-2011, National Cancer Institute. Bethesda, MD, http://seer.cancer.gov/csr/1975_2011/, based on November 2013 SEER data submission, posted to the SEER web site, April 2014.
6. Majumdar, Sumit R., Robert H. Fletcher, and Arthur T. Evans. "How does colorectal cancer present? symptoms, duration, and clues to location."*The American journal of gastroenterology* 94.10 (1999): 3039-3045.
7. WANG, THOMAS D., and JACQUES VAN DAM. "Optical Biopsy: A New Frontier in Endoscopic Detection and Diagnosis." *Clinical gastroenterology and hepatology : the official clinical practice journal of the American Gastroenterological Association* 2.9 (2004): 744–753. *PMC*. Web. 6 Apr. 2015.
8. Elahi, Sakib F., and Thomas D. Wang. "Future and advances in endoscopy."*Journal of biophotonics* 4.7-8 (2011): 471-481.
9. Thiberville L, Sala ¨un M, Lachkar S, Dominique S, Moreno-Swirc S, VeverBizet C, Bourg-Heckly G. Confocal fluorescence endomicroscopy of the human airways. Proc Am Thorac Soc 2009;6:444–449.
10. Branzan AL, Landthaler M, Szeimies RM. In vivo confocal scanning laser microscopy in dermatology. Lasers Med Sci 2007;22:73–82.
11. Thong PS, Olivo M, Kho KW, Zheng W, Mancer K, Harris M, Soo KC. Laser confocal endomicroscopy as a novel technique for fluorescence diagnostic imaging of the oral cavity. J Biomed Opt 2007;12:014007.
12. Goetz M, Kiesslich R. Confocal endomicroscopy: in vivo diagnosis of neoplastic lesions of the gastrointestinal tract. Anticancer Res 2008;28:353–360.

13. Kiesslich, Ralf, et al. "Confocal laser endoscopy for diagnosing intraepithelial neoplasias and colorectal cancer in vivo." *Gastroenterology* 127.3 (2004): 706-713.

14. Muldoon TJ, Roblyer D, Williams MD, Stepanek VM, Richards-Kortum R, Gillenwater AM. Noninvasive imaging of oral neoplasia with a high-resolution fiber-optic microendoscope. Head & Neck. 2012;34(3):305-12. PMCID: 3078517

15. Pierce, Mark, Dihua Yu, and Rebecca Richards-Kortum. "High-Resolution Fiber-Optic Microendoscopy for *in Situ* Cellular Imaging." *Journal of Visualized Experiments : JoVE* 47 (2011): 2306. *PMC*. Web. 3 Mar. 2015.

16. Muldoon TJ, Pierce MC, Nida DL, Williams MD, Gillenwater A, Richards-Kortum R. Subcellular-resolution molecular imaging within living tissue by fiber microendoscopy. Opt Express. 2007;15(25):16413-23.

17. S. Prieto, A. Powless, A. Majid, J. Laryea, J. Mizell, S. Sharma, and T. Muldoon, "Fiber Bundle Microendoscopy for Characterization of Dysplastic Lesions in Colonic Epithelium," in Biomedical Optics 2014, OSA Technical Digest (online) (Optical Society of America, 2014), paper BT3A.14.

18. http://www.pages.drexel.edu/~sis26/MosaickingTutorial.htm